

Towards integrative computational materials engineering of steel components

G. J. Schmitz · S. Benke · G. Laschet · M. Apel · U. Prahl · P. Fayek ·
S. Konovalov · J. Rudnizki · H. Quade · S. Freyberger · T. Henke ·
M. Bambach · E. A. Rossiter · U. Jansen · U. Eppelt

Received: 3 February 2011 / Accepted: 29 April 2011 / Published online: 13 May 2011
© German Academic Society for Production Engineering (WGP) 2011

Abstract This article outlines on-going activities at the RWTH Aachen University aiming at a standardized, modular, extendable and open simulation platform for materials processing. This platform on the one hand facilitates the information exchange between different simulation tools and thus strongly reduces the effort to design/re-design production processes. On the other hand, tracking of simulation results along the entire production chain provides new insights into mechanisms, which cannot be explained on the basis of individual simulations. Respective simulation chains provide e.g. the basis for the determination of materials and component properties, like e.g. distortions, for an improved product quality, for more efficient and more reliable production processes and many

further aspects. After a short introduction to the platform concept, actual examples for different test case scenarios will be presented and discussed.

Keywords ICME · Phase-field modeling · Through-process simulation · Multi-scale modeling · Steel processing · Integrative computational materials engineering · Simulation platform · Microstructure evolution · Effective properties

1 Introduction

Any production is based on materials which eventually become components of a final product. Materials properties thus are of great importance for productivity and robustness of processing during production as well as for application and reliability of the final product components. Permanently increasing complexity of products and their manufacturing processes combined with the demand on high quality products with tight dimensional and material quality tolerances require the use of integrative simulation techniques in product and process design. This situation leads to a dilemma, where more and more effort has to be spent in planning in order to meet the challenges of producing a high value product. Strategies to reduce the polylemma of production are addressed within the Cluster of Excellence “Integrative Production Technologies for High Wage Countries” [1].

Nowadays simulations form an integral part of the planning activities for production processes. To decrease the dilemma between the efforts spent for planning and the product value eventually being generated, a reduction of planning efforts and an increased value of a product are possible approaches, Fig. 1.

G. J. Schmitz (✉) · S. Benke · G. Laschet · M. Apel
Access e.V. at the RWTH Aachen, Intzestr. 5,
52072 Aachen, Germany
e-mail: G.J.Schmitz@access.rwth-aachen.de

U. Prahl · P. Fayek · S. Konovalov · J. Rudnizki · H. Quade
Department of Ferrous Metallurgy, RWTH Aachen,
Intzestr. 1, 52072 Aachen, Germany

S. Freyberger
Foundry Institute, RWTH Aachen, Intzestr. 5,
52072 Aachen, Germany

T. Henke · M. Bambach
Institute of Metal Forming, RWTH Aachen,
Intzestr. 10, 52072 Aachen, Germany

E. A. Rossiter
Welding and Joining Institute, RWTH Aachen,
Pontstr. 49, 52062 Aachen, Germany

U. Jansen · U. Eppelt
Fraunhofer Institute for Laser Technology,
Steinbachstr. 14, 52074 Aachen, Germany

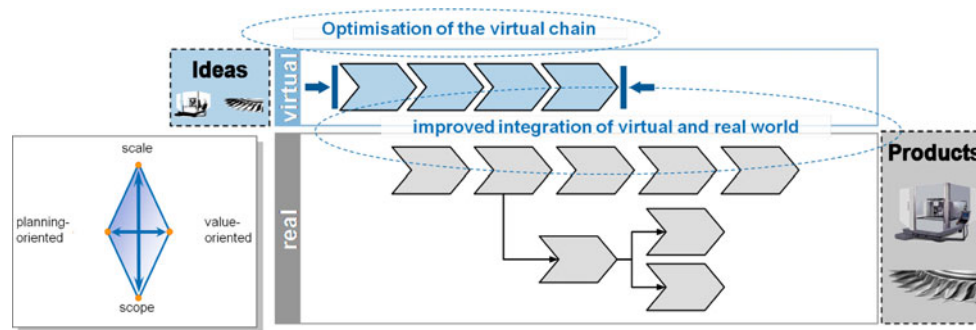


Fig. 1 Planning efforts can be strongly reduced with respect to time and costs (1) if the performance of individual simulation processes is increased, (2) if only those models relevant to mimic the desired effect in sufficient detail are used and especially (3) if the information

exchange between individual models is improved by standardized interfaces. Simulating the entire production chain also leads to an increased value of the products e.g. by a future prediction of their life-cycle

The major objective of this article is the description of a virtual, integrative numerical approach for the simulation of materials processing and of the microstructure evolution along the entire production chain. This approach eventually allows for prediction of effective materials properties from calculated microstructures and provides tools for an extraction of relevant data adapted to the requirements of higher level simulation codes. Further it enables the integration of materials processing models into production and machinery models and eventually the extension of the simulations towards a life-cycle prediction of the component. The long term objective is to provide companies with a toolbox allowing to optimize and adjust their processes and products dependent on the specifications of the materials and the actual process conditions and thus to enable dynamic reactions to an evolving market. The platform shall moreover be used as an educational tool for metallurgists, mechanical engineers and production engineers allowing for an integrative view on processes and products.

2 Integrative computational materials engineering platform

ICME—Integrative Computational Materials Engineering—has been identified as a strategic approach for future competitiveness [2]. ICME in the first place requires an efficient exchange of information between a variety of different available commercial and/or academic simulation tools. Based on previous work on integrative materials modeling [3], a modular, open and standardized simulation platform concept has been defined [4]. This platform provides a toolbox being adaptable to specific production scenarios and being extendable to future and more detailed models allowing for an improved predictive quality. To realize such a platform concept several software codes and models for materials processing available at the RWTH

Aachen University have been adapted to a common standard based on the VTK format [5, 6] and using semantic approaches [7] allowing for an efficient information exchange between the process simulation tools along the process chains and also across several length and time scales, Fig. 2.

Workflow sheets for process chains can be edited and the simulations then be performed on a computational GRID in the internet using a middleware [8].

In the following sections, the process chains for the production of a line pipe, a transmission component and a bearing housing are introduced as test cases to demonstrate the platform performance. Other applications such as a polymer component (top-box) and a textile reinforced piston rod will be described elsewhere [9, 10]. Different heterogeneous process simulation tools have been daisy-chained on the basis of the defined common standard to allow for simulation of a variety of processes occurring in these process scenarios. The simulation tools being applied cover the description of the entire production chain starting from casting of a homogeneous melt, heat treatments, hot and cold forming, machining and joining processes up to simulation of a load history arising during operation.

3 Line-pipe

Strength and toughness of line-pipe materials are mainly influenced by their microstructure, which in turn is determined by processing and alloy composition. For the test-case “Line-pipe” a through process simulation chain has been established for a steel of the grade X65 both on the macroscopic process scale and on the scale of the microstructure. The processes being considered are heat-treatments, hot rolling, machining, U- and O-forming and welding. Eventually, estimates for the strength and toughness of the material are derived.

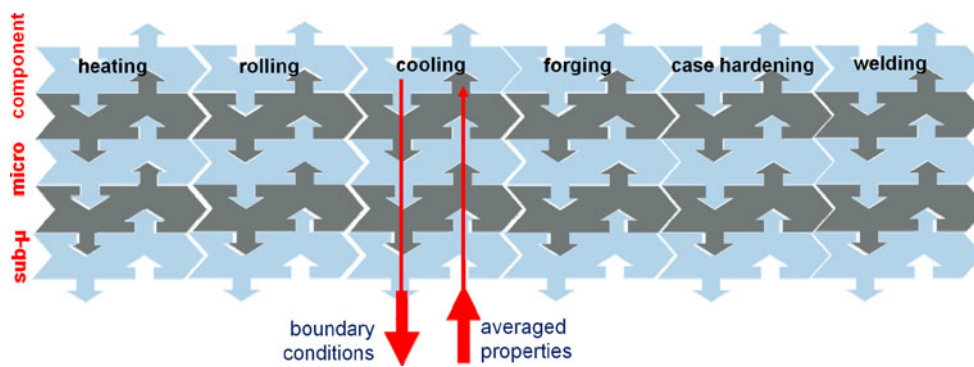


Fig. 2 Modular concept of the AixViPMaP[®] simulation platform. Individual simulation tools being considered as *black-boxes* can be combined for different processes along the entire production chain on different length scales. Higher level simulation codes provide boundary conditions for simulations on a smaller scale. Properties

being determined at a small length scale are homogenized/averaged and fed back to the higher level codes. The dark modules represent interface routines allowing bridging the scales like e.g. homogenisation models

Heat treatment processes in general involve the steps of heating a component, dwelling it at defined conditions (temperature, time and atmosphere) and subsequent cooling. These basic steps may be combined to describe more general heat-treatment schemes. Heat treatment processes on the macro scale have been simulated using the software CASTS [11], which allows for the simulation of solidification and thermo-mechanical processes. This software has been further extended for the description of solid phase transformations [12] and of grain growth phenomena, which are described on the basis of the Leblond model [13]. The temperature–time history of different integration points, i.e. characteristic locations or critical areas of the component, has been extracted from the macro simulations and transferred as boundary conditions to simulations of the microstructure evolution at these locations. This microstructure evolution is then modelled using the multiphase field code MICRESS[®], which is coupled to thermodynamic databases [14]. The simulated microstructure domain eventually constitutes a Representative Volume Element (RVE) for a subsequent determination of the effective properties at the selected location, Fig. 3.

The geometry/mesh of the slab and the local distributions of temperature, phase fractions, concentration etc. resulting from the heating process are forwarded to the following hot rolling simulation Fig. 4.

The *hot rolling process* is simulated using the finite element code LARSTRAN/-shape coupled with the software StrucSim [15]. LARSTRAN and StrucSim are capable of describing both the macroscopic forming process as well as microstructural phenomena, such as dynamic and static recrystallisation and grain growth using a mean field approach. Hot rolling of a line-pipe steel is typically performed in pass schedules which can involve 10–20 rolling passes. For individual passes, the rolling stock may be rotated by 90 degrees, rolled along the width direction, and rotated back for subsequent passes. The finite element model StrucSim as an integrated microstructure model allows for the simulation of the complete pass schedule of the rolling stock taking into account the evolution of microstructure during hot rolling. This approach allows for accurate roll force predictions as well as the prediction of properties such as grain size distributions after rolling, while at the same time being computationally efficient.

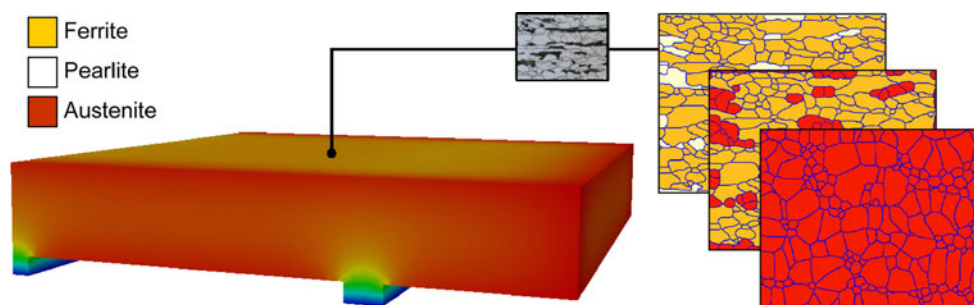


Fig. 3 Principle of the coupled macro and micro heat treatment simulations. The supporting rails and the geometry dependant heat radiation lead to an inhomogeneous temperature distribution in the slab during the heating process. The slab may furthermore reveal

macrosegregation patterns originating from the continuous casting process. Both types of inhomogeneities affect the subsequent microstructure evolution at characteristic points

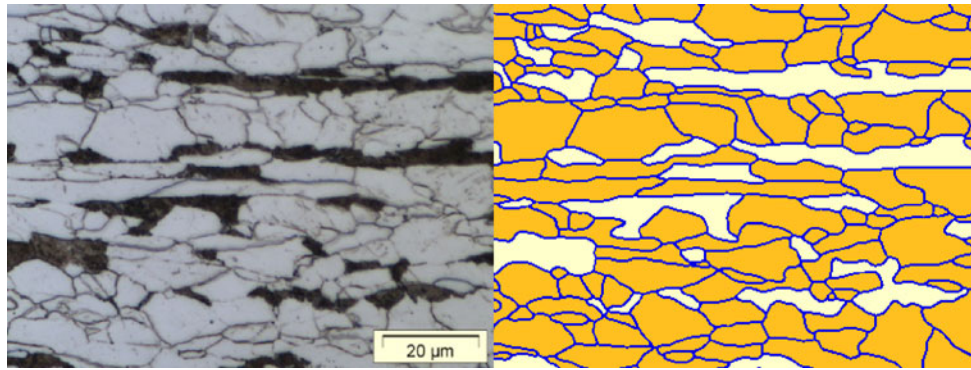


Fig. 4 Real micrograph (left, dark: pearlite, grey: ferrite) and digitalized microstructure entered into MICRESS® (right, dark: ferrite, light: pearlite). A full simulation of the evolution of this

microstructure starting from the homogeneous melt can be replaced by including experimental microstructures at a later stage of the process chain as an initial condition into the simulation chain

The subsequent cooling process is again simulated with CASTS. Special features like e.g. quenching of the rolled sheet may be modeled here as well.

The **machining process** for preparation of the welding grooves is considered as a simple removal of mesh elements accompanied by a redistribution of stresses and strains in the component and is also modeled using CASTS.

The **“U”- and “O”-forming process steps** are modeled using the finite element program ABAQUS [16], which requires both the geometry of the rolled sheet and especially the local materials properties. While the geometry and other information are taken from the previous cooling simulation, the effective materials properties, especially the flow curves, have to be determined from the local microstructure using a multi-scale simulation approach.

The multi-scale simulation allows for predicting material properties e.g. the flow behavior of a multiphase steel microstructure. These properties are derived from the knowledge of the properties of the individual phases and their topological arrangement. Three scales have been distinguished in the case of the X65 line-pipe steel: the micro-scale of a ferrite/cementite bilamella representing

the pearlite phase; the meso-scale with a Representative Volume Element (RVE) of pearlite inclusions in a ferrite matrix and the macro-scale with the entire sheet metal and the tools, Fig. 5.

The mathematical homogenization tool HoMat [17] at first evaluates the effective thermoelastic properties of the pearlite bilamella formed by a ferrite and cementite layer. As pearlite exhibits a large stiffness, this phase is assumed to have a pure elastic material behaviour. The calculation takes into account cubic elastic properties for the ferrite phase. The elastic properties of the orthorhombic cementite phase are deduced from ab initio calculations by Nikolussi et al. [18]. A crystallographic orientation relationship between ferrite and cementite within pearlite is also taken into account. Zhang et al. [19] reported that hypoeutectic steels, like the analysed X65, only show the Isaichev orientation relationship, which accordingly was used in the calculations.

The elasto-plastic law adopted for the ferrite matrix is based on a flow curve model of Rodriguez and Gutierrez [20]. Based on experimental micrograph observations, a reference RVE containing 14% of pearlite phase ($V_f = 14\%$) is generated. This volume fraction is

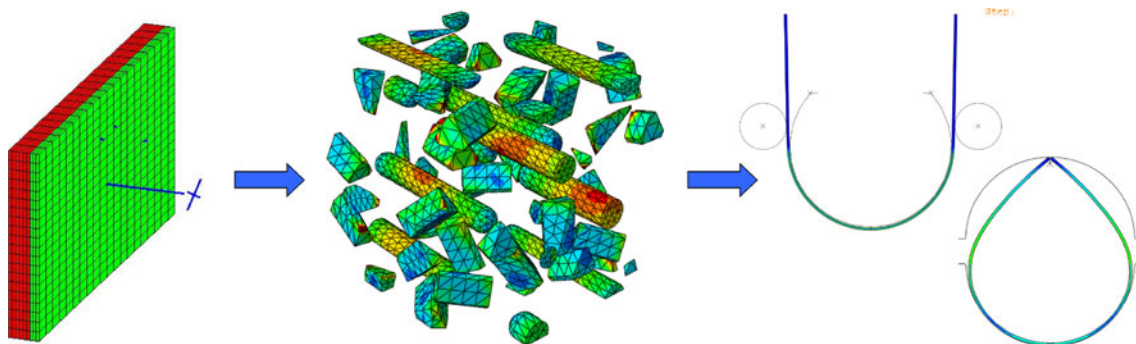


Fig. 5 The three scales of the multi-scale simulation, left: bilamella (width $\lambda = 330$ nm) of pearlite consisting of cementite (bright) and ferrite (dark), middle: RVE of pearlite in a ferrite matrix (not displayed) and right: macroscopic sheet of X65 steel during U- and O-forming

composed of small prismatic pearlite (7.2%) and of elongated pearlite sphero-cylinders (6.8%), Fig 6. In order to investigate the influence of a different pearlite content at different locations of the sheet, two additional RVE's are generated with $V_f = 10\%$ and $V_f = 7\%$ respectively. For these RVE's uniaxial tensile tests have been performed in order to deduce the effective non-linear stress–strain curves of the ferrite-pearlite microstructure for different loading directions [21, 22], Fig. 7.

First results show that a higher strength is obtained in rolling direction (X) than in the transverse directions. Due to random generation of small prismatic pearlite, similar flow curves are obtained for the Y and Z directions, leading to a transverse isotropic material behaviour. A significant deviation from experimental data has however to be noted. Similar discrepancies between experiment and simulation are also observed by Guitierrez and Altuna [23] for different low carbon steels. Indeed, the experimental curve exhibits a yield point elongation, produced by Lüders band formation due to dynamic strain ageing coupled to interstitials in solid solution. Such ageing effects are not described by the Rodriguez and Gutierrez model. Thus, there exists a

high degree of uncertainty of the flow curve for ferrite at low strains, due to iron's acute sensitivity to ageing.

For larger strains the predicted curves moreover present larger work hardening as compared to the experimental observations. This deviation may be related to (1) the idealized shape and orientation of the pearlite (2) the assumption of a fully elastic behaviour of the pearlite phase, (3) to the absence of an initial stress/strain state resulting from the preceding process steps and (4) to the cementite Hooke matrix being extrapolated from ab initio calculations at $T = 0$ K to room temperature. In order to improve the flow curve predictions, a stochastic analysis with the random generation of more than 30 RVE's containing elasto-plastic pearlite of different shapes/orientations and revealing residual stresses is currently under investigation.

A relative decrease of 10% in strength is observed for RVE-2 ($V_f = 10\%$) and 17.5% for RVE-3 ($V_f = 7\%$) respectively. The three flow curves for these different pearlite contents (corresponding to different sheet locations) are eventually introduced in the forming simulations to take the effect of local variations of pearlite volume

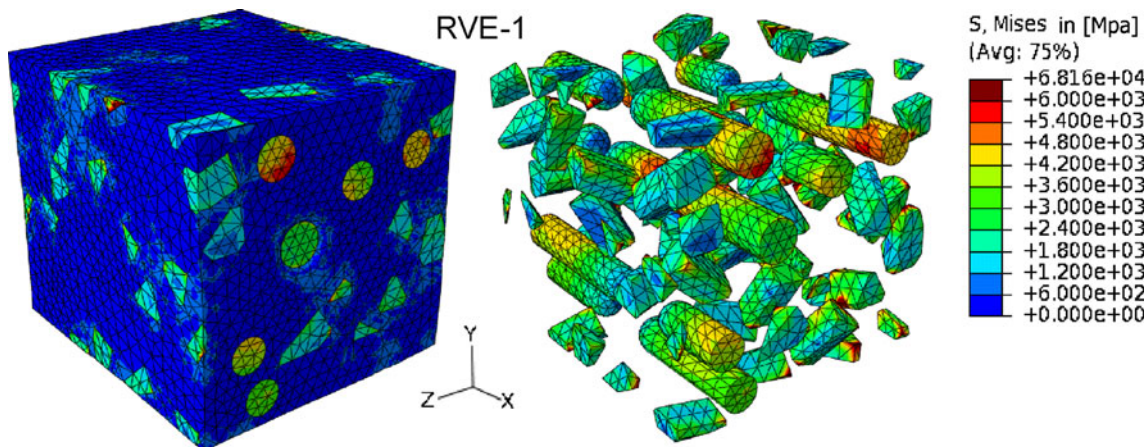
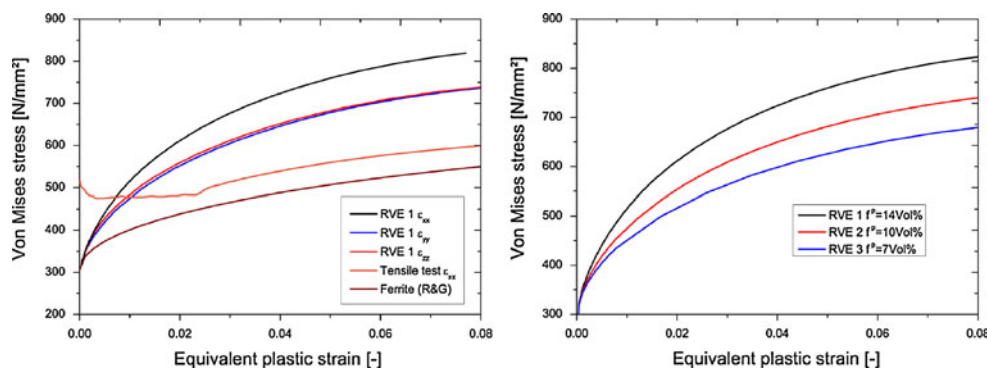


Fig. 6 Uniaxial virtual extension test of the reference RVE with a pearlite content of 14.1% ($\epsilon_{xx} = 0.07$). Von Mises stresses on the entire RVE (left) and in the pearlite (right) are shown

Fig. 7 Flow curves of RVE 1 ($V_f = 14\%$) tested in X,Y and Z directions and compared to an experimental flow curve in x direction and including the flow for ferrite as adapted from Rodriguez and Gutierrez [20] (left) and flow curves for different RVE with different volume fractions of pearlite tested in x-direction (right)



fractions on the macroscopic distribution of stresses and strains into account [20, 21].

The **welding process** on the macro-scale is simulated using SimWeld [24] and SYSWELD [25]. While SYSWELD is applied for the calculation of residual stresses in the line-pipe tube and respective distortions, SimWeld calculates the heat input, the heat distribution, the weld pool geometry, the size of the heat affected zone and the weld seam geometry. The joint geometry is taken from the preceding O-forming process simulation results. Thermo-magnetic properties of the base material as well as those of the flux and the wire are accounted for in this simulation. Respective properties are taken from the SimWeld material data base. The weld process is calculated as a stationary process with the power input being calculated based on voltage and current.

The results of the welding process simulation are used as input for SYSWELD for further modeling distortion and residual stress of the line pipe. The weld seam geometry is transferred from SimWeld to SYSWELD using the tool SW2SW [26], which allows to insert the weld seam geometry into the line-pipe mesh. The residual stress state of the material before welding is taken from the preceding O-forming simulation. Deformations and residual stresses after welding can thus be modeled taking into account the residual stress state before welding and the work piece geometry including the weld seam.

The weld seam commonly forms the weakest part of a component and often leads to failure due to a reduced toughness of the weld affected area. During welding, the microstructure is significantly modified. Its evolution is simulated on the micro-scale with the phase-field code MICRESS[®] both in the weld pool and in the heat affected zone [27] (Fig. 8). Characteristic integration points in the weld pool and in the heat affected zone are considered and their temperature–time histories are extracted and transferred into the simulations on the micro-scale.

This novel approach allows the description of several phenomena: during O-forming the sheet edges are cold-formed leading to a local increase of the dislocation density. High dislocation densities promote local recrystallisation and thus influence the resulting grain size. The recrystallized grains serve as seeds and thus provide boundary conditions for modeling the dendritic solidification of the weld pool. Grain growth and solid state transformation processes are modeled in the heat affected zone. By now, the presented approach thus allows for estimates of the grain size in the weld pool and the heat affected zone. The resulting grain size, which has a major influence on the material's toughness, can be used to qualitatively estimate the degradation caused by the welding process.

4 Transmission component

Increasing the efficiency for the production of gear wheels as well as improving their quality in application is of major importance for increased competitiveness. Raising the carburizing temperature would shorten the heat treatment process. A temperature increase, however, to some extent will be limited by furnace capabilities, but -more important- by a suitable control of the grain size at high temperatures. The final grain size has a major influence on the life time of the hardened components [28, 29] and the grain size stability during high temperature case hardening can be improved by adding micro alloying elements. The efficiency of such alloy modifications for grain boundary pinning strongly depends on the entire manufacturing route and the respective process parameters. Additional alloy elements and the manufacturing process chain thus have to be optimized in parallel [30, 31].

Moreover, distortions after hardening of the component can lead to major costs due to additional finishing procedures or high scrap rates. Such distortions are mostly

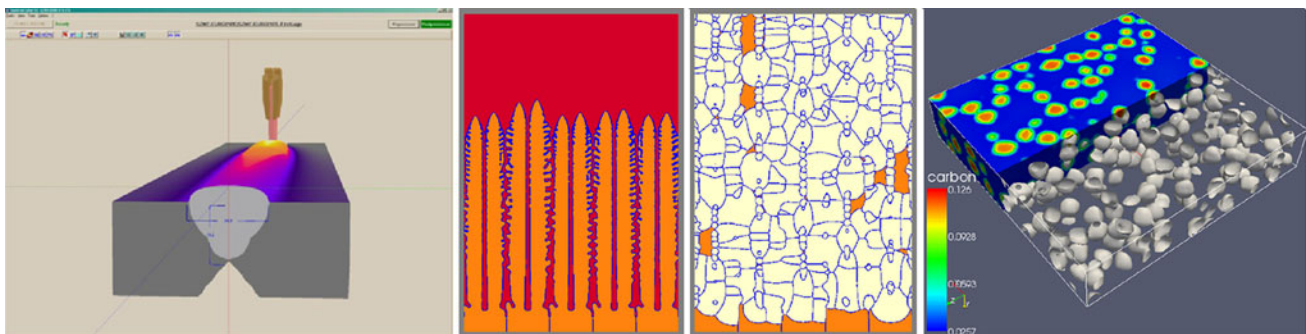


Fig. 8 Weld seam geometry calculated using SimWeld (*left*). The temperature evolution is used as boundary condition for modelling the dendritic solidification of δ -ferrite in the joint (*middle, left*), subsequent formation of austenite (*middle, right*) as well as phase-

transformations, recrystallisation and grain growth in the heat affected zone (*right*, depicted are carbon and α -phase distributions during the γ - α transition)

caused by inhomogeneities due to segregation of alloying elements, by inhomogeneous grain size distributions or by an unfavorable heat distribution in the component either due to its shape or to the heating conditions [32, 33, 34].

The process parameters for both simulation and experimental verification in this test case were adjusted close to industrial parameters. The investigated material 25MoCr4 belongs to a typical microalloyed case hardening steel for high temperature case hardening.

During the hot rolling a cast slab is shaped into a round bar. The initial microstructure by now is not calculated but assumed to be homogeneous. The consideration of macrosegregation originating from the continuous casting process and the formation of banded structures both influencing distortions of the final gear wheel will be investigated in the future. The preliminary shape of the gear component is then obtained by a forging process and its final shape is reached by machining, which requires a pearlitic-ferritic microstructure to enhance machinability. This microstructure can be realized by the special FP- (“Ferrite-Pearlite”) annealing. The case hardening process step increases the hardness and wear resistance of the surface of the component while maintaining a ductile core. During subsequent laser beam welding an additional part can be joined to the gear component thus forming an assembled product, Fig. 9.

Scopes of the integrative simulation approach are (1) minimization of the experimental effort to develop relevant processes (2) identification of all process parameters especially with respect to an improved grain size control during high temperature case hardening and (3) optimization of the process chain in terms of energy, cycle times and costs.

After definition of the initial state and calculation of the initial conditions, the simulation of the first hot forming process steps is carried out. On the macro level, the hot rolling as well as the hot forming simulation is split on three steps, heating—deformation—cooling, as for the calculation of these process steps two different simulation tools are needed. The calculation of the heating and cooling including phase transformation is done by CASTS [11], [12] and the forming simulation at high temperature is performed using LARSTRAN/shape [15]. The results of the calculation can be transferred to the meso- and micro levels and to subsequent process steps. The heat distribution and phase transformations during the heat treatment like FP-annealing and high temperature case hardening can be calculated on the component scale by means of CASTS using empirical approaches [35]. The temperature history at specific integration points is used as boundary condition by MICRESS® for calculating the phase transformation and microstructure development on the basis of physical

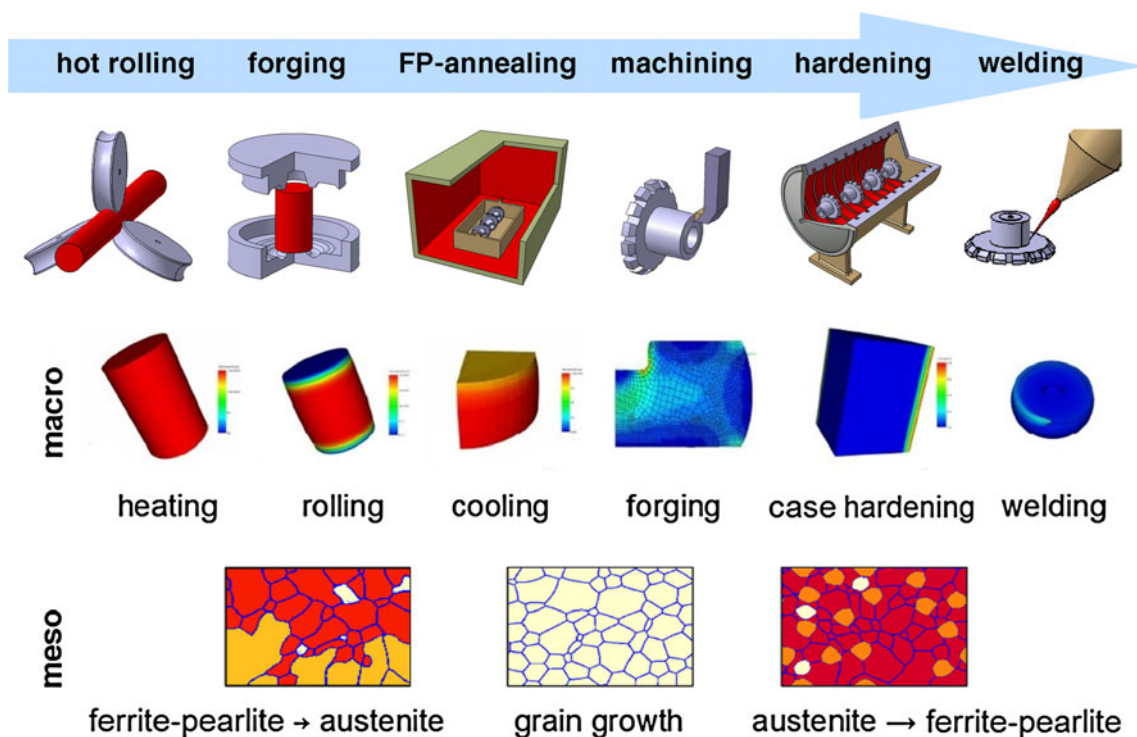
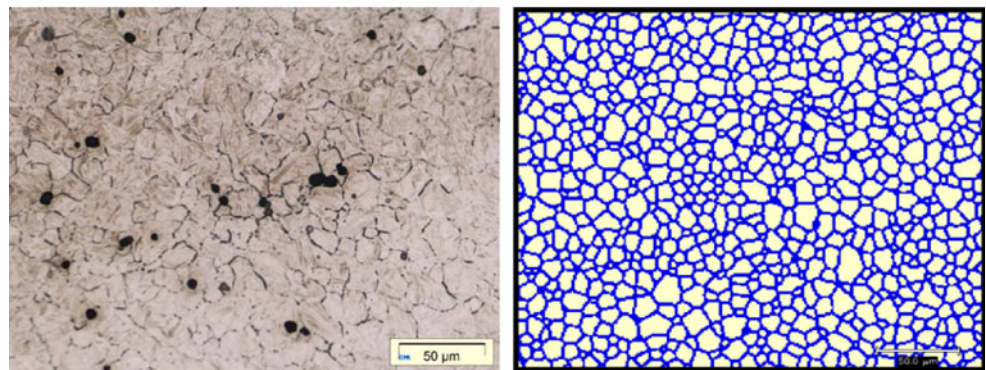
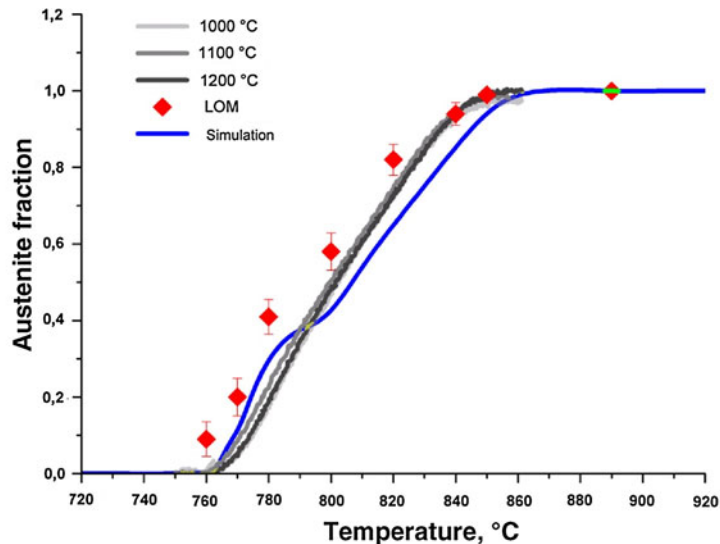


Fig. 9 Typical process chain for transmission components and examples of the simulation results for a treatment of a simplified shape of a transmission component on the macro scale along the process chain as well as the simulation for the phase transformation on the meso scale

Fig. 10 Comparison of the simulations with experimental (*LOM* light optical microscopy) and dilatation results for austenite formation from a ferritic-pearlitic structure (*top*) and comparison of simulated and experimental austenitic microstructure at carburization temperature (*bottom*)



models, Fig. 10. The evolution of the precipitate distribution during the different heat treatments is calculated on the microscale using MatCalc [36] and then used to calculate an effective Zener force. This effective Zener force enters into the MICRESS[®] simulations, where it reduces the grain boundary mobilities and accordingly affects grain growth [37]. Phenomena like abnormal grain growth can be tackled this way [38].

For the modeling of laser welding as the last process step, two components have to be merged into one mesh. The laser weld process then is simulated using the Laser-Weld3D program [39]. The temperature distribution in the welded components then may eventually be used to calculate distortions evoked by the welding process.

5 Bearing housing

This testcase addresses the integrative simulation of the manufacturing process chain and the life time behavior of a bearing housing which is a high-precision cast part made from austenitic stainless steel (GX5CrNiMoNb19-11-2). Coupled simulations on two length scales have been

performed, Fig. 11. The macroscopic simulation of the manufacturing process uses sequential coupling of the commercial FV solidification software Magma [40] and the FE codes CASTS [11, 12] and Abaqus [16]. On the microscale a multi-phase-field model [14] is used to calculate the dendritic solidification morphology and evolution of the corresponding micro-segregation pattern during solidification and heat treatment. The combination of residual stresses and the local microsegregation pattern originating from the initial solidification might evoke highly localized martensitic transformations which eventually will lead to a deformation during service life and accordingly to the failure of the component.

Bridging from the process simulation scale to the scale of the microstructure simulation is again realized by the use of the temperature history and effective compositions at dedicated points of the component. The calculated microstructure provides the basis for the modeling of the deformation induced martensitic transformation in the chromium enriched and nickel depleted regions observed on the microscale. By the use of virtual testing methods [41], [42], the effective mechanical properties of the microstructure after the martensitic transformation are

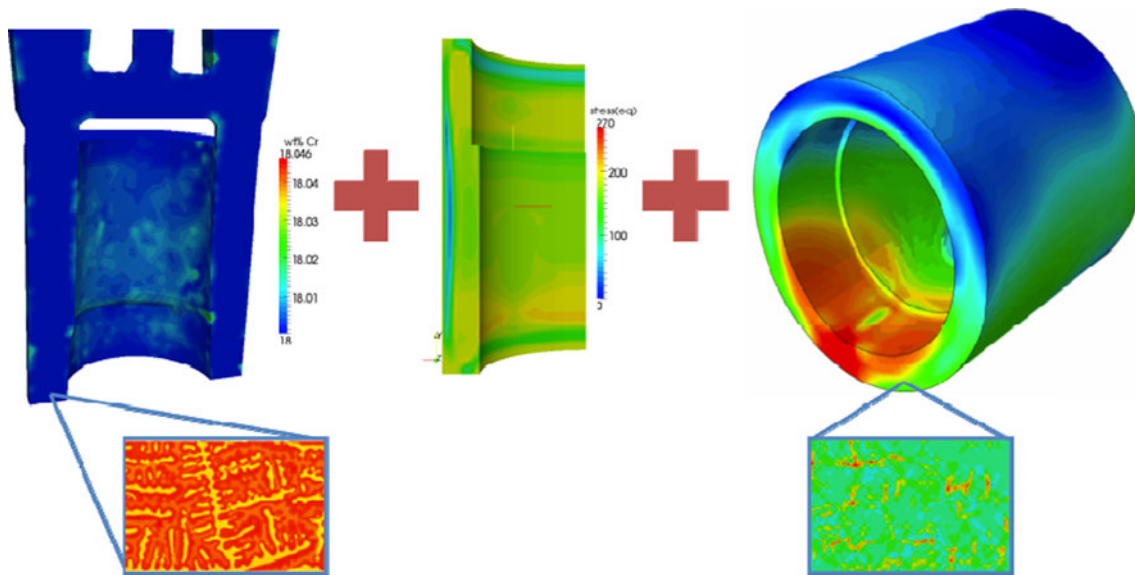


Fig. 11 Segregation of chromium after casting on the macro- and micro levels (*left*) and internal stresses after machining (*middle*) being superimposed by a point-like service load acting on the bearing housing (*right*) eventually lead to a localized martensitic transformation

determined and coupled back to the macroscopic simulation of the life time behavior of the machine part. The simulation results are compared to experimental findings in order to validate the integrative model.

Only a combined consideration of effects throughout the process chain on two length-scales allows the description of the observed distortions arising during operation of the component. The microstructure and especially segregation patterns are largely determined during solidification influencing the local stability of martensite and thus influencing mechanical properties like the local yield strength on the macro scale. The influence of heat-treatment imposed internal stresses and their rearrangement during machining can, in this case, be described on a macroscopic scale. Loads during service superimpose these internal stresses leading to a plastic strain especially close to regions of delta-ferrite (micro-scale) and thus to a local transformation of austenite to martensite going along with a change in volume of about 3% and respective distortions.

6 Future perspectives

This paper has summarized the present status of a virtual platform for the simulation of materials processing. The nucleus of this platform is based on simulation tools available at the RWTH Aachen University, but it is meant to be extendable and open to any interested user and provider of simulation models in future. A standardization approach has been identified as a key component for establishing such a simulation platform. First results on integrative simulations of dedicated testcase scenarios for

steel components have been depicted and reveal that specific properties resp. phenomena can only be understood in the frame of a holistic approach covering several process steps on both the process scale and the scale of the microstructure.

Future activities will aim at improving the predictive capabilities of both the individual models and of their coupled use, at including further testcases comprising other products and other materials. Further activities will relate to including new tools into the platform to cover further aspects of the product life-cycle like models for machining, for operational conditions, for rework and repair and eventually for recycling. Further extensions will relate to an inclusion of product design models and even of logistic aspects affecting the product properties.

Acknowledgments The present article is based on on-going work of a consortium of the following institutes at the RWTH Aachen University: Foundry Institute (GI), Institute for Ferrous Metallurgy (IEHK), Welding and Joining Institute (ISF), Surface Engineering Institute (IOT), Institute for Metal Forming (IBF), Institute for Plastics Processing (IKV), Institute for Scientific Computing (SC), Department of Information Management in Mechanical Engineering (ZLW/IMA), Institute for Textile Technology (ITA), Fraunhofer Institute for Lasertechnology (ILT/NLD) and ACCESS. Funding of the depicted research by the German Research Foundation (DFG) in the frame of the Cluster of Excellence “Integrative Production in High Wage Countries” is gratefully acknowledged.

References

1. www.production-research.de
2. National research council (2008) :integrated computational materials engineering: a transformational discipline for improved

- competitiveness and National security; National Academic Press, Washington, DC ISBN: 0-309-12000-4
3. Gottstein G (ed) (2007) Integral materials modelling: towards physics based through-process models, Wiley—VCH Verlag, Weinheim. ISBN:978-3-527-31711-0
 4. Schmitz GJ, Prah U (2009) Toward a virtual platform for materials processing. *JOM* 61(5):26
 5. Schroeder W, Martin K, Lorensen B (2006) The visualization toolkit—an object-oriented approach to 3D Graphics, 4th Ed, Kitware, Inc. www.vtk.org
 6. Benke S et al Definition of a standardized data format for the exchange of simulation data. Available online at: www.aixvipmap.de
 7. Schilberg D, Gramatke A, Henning K (2008) Semantic interconnection of distributed numerical simulations via SOA. Proceedings of the world congress on engineering and computer science, San Francisco, USA, pp 894–897. ISBN:978-988-98671-0-2
 8. Cerfontaine P, Beer T, Kuhlen T, Bischof C (2008) Towards a flexible and distributed simulation platform computational science and its applications—ICCSA, Springer lecture notes in computer science LNCS 5072 Part1
 9. Arping T, Heesel B, Kashko T, Laschet G, Baranowski T (To be published)
 10. Kuckhoff B, Benke S, Kashko T (To be published)
 11. Benke S, Laschet G (2008) On the interplay between the solid deformation and fluid flow during solidification of a metallic alloy. *Comput Mat Sci* 43(1):92
 12. Benke S, Rudnizki J, Suwanpinij P, Prah U (2008) Modeling hot rolling: a study on the microstructural changes during the Austenite to Ferrite phase transformation in dual phase steels. Presented at 8th World congress on computational mechanics (WCCM8), June 30–July 5 Venice, Italy
 13. JB Leblond et al (1984) *Acta Metall* 32:137
 14. MICRESS®: The MICROstructure evolution simulation software: <http://www.micress.de>
 15. Kopp R, Horst C (2004) Modelling of elastic effects in forming processes. Particularly the rolling process. *AIP Conf Proc* 712:375–381
 16. Abaqus, Dassault Systèmes Simulia Corp. (2009) Standard user manual, version 6.9, Hibbit, Karlsson and Sorensen, Providence, RI, USA
 17. Laschet G, Apel M (2010) Thermo-elastic homogenization of 3-D steel microstructure simulated by phase-field method. *Steel Res Int* 81(8):637
 18. Nikolussi M (2008) Extreme elastic anisotropy of cementite, Fe₃C: First-principles calculations and experimental evidence. *Scripta Mater* 59:814–817
 19. Zhang MX, Kelly PM (1997) Accurate orientation relationships between ferrite and cementite in pearlite. *Scripta Materialia* 37(12):2009
 20. Rodriguez R, Gutierrez I (2003) A unified formulation to predict the tensile curves of steels with different microstructures. *Materials Science Forum* 426–432:4525
 21. Laschet G, Quade H, Henke T, Dickert HH, Bambach M (2010) Comparison of elasto-plastic multi-scale analyses of the U-forming process of a steel line-pipe tube, In: Proceedings of the IV European Conference on Computational mechanics, Paris, France
 22. Quade H, Fayek P, Laschet G, Henke T (2010) Multi-scale Simulation of the U- and O-forming of a Line-pipe Tube. Presented at the First Conference on Multiphysics Simulation, Bonn, Germany to appear in “Int J Multiphys”
 23. Gutierrez I, Altuna MA (2008) Work-hardening of ferrite and microstructure-based modeling of its mechanical behaviour under tension. *Acta Mater* 56:4682
 24. Bleck W, Reisgen U, Mokrov O, Rossiter E, Rieger T (2010) Methodology for Thermomechanical Simulation and Validation of Mechanical Weld-Seam Properties. *Adv Eng Mater* 12(3):147–152
 25. Rieger T, Gazdag S, Prah U, Mokrov O, Rossiter E, Reisgen U (2010) Simulation of Welding and Distortion in Ship Building. *Adv Eng Mater* 12(3):153–157. <http://www.esi-group.com/products/welding>
 26. Reisgen U, Schleser M, Mokrov O, Ahmed E, Schmidt A, Rossiter E (2009) Integrative Berechnung von Verzug und Eigenspannung auf Basis realer Schweißparameter. Presented at SYSWELD Forum, Weimar, Germany
 27. Apel M, Böttger B (2009) Phase-field simulation of the microstructure formation in the weld pool and in the heat affected zone during welding of steel. Presented at the 2nd symposium on phase-field modelling in materials science, Aachen
 28. Grosch J, Liedtke D, Kallhardt K, Tacke D, Hoffmann R, Luiten CH, Eysell FW (1981) Gasaukohlern bei Temperaturen oberhalb 950°C in konventionellen Öfen und in Vakuumöfen. *HTM Härtereitechn Mitt* 36(5):262
 29. Pacheco JL, Krauss G (1990) Gefüge und Biege-wechselfestigkeit ein-satzgehärteter Stähle. *HTM Härtereitechn Mitt* 45(2):77
 30. Hippenstiel F, Bleck W, Clausen B, Hoffmann F, Kohlmann R (2002) Innovative Einsatzstähle als maßgeschneiderte Werkstofflösung zur Hochtemperatur-aufkohlung von Getriebekomponenten. *HTM Härtereitechn Mitt* 27(4):290–298
 31. Klenke K, Kohlman R (2005) Einsatzstähle in ihrer Feinkornbeständigkeit, heute und morgen. *HTM Z Werkst Wärmebehand Fertigung* 60(5):260
 32. Kleff J, Hock S, Kellermann I, Fleischmann M, Küper A (2005) Hochtemperatur-Aufkohlern: Einflüsse auf das Verzugsverhalten schwerer Getriebebauteile. *HTM Z Werkst Wärmebehand Fertigung* 60(6):311
 33. Wise JP, Matlock DK (2000) Bending Fatigue of Carburized Steels: a statistical analysis of process and microstructural parameters. SAE 2000 World Congress, Detroit
 34. Prinz C, Clausen B, Hoffmann F, Kohlmann R, Zoch HW (2006) Metallurgical influence on distortion of the case-hardening steel 20MnCr5. *Materialwissenschaft und Werkstofftechnik* 37(1):29
 35. Rudnizki J, Zeislmair B, Prah U, Bleck W (2010) Thermodynamical simulation of carbon profiles and precipitation evolution during high temperature case hardening. *Steel Res Int* 81(6):472
 36. Kozeschnik E, Svoboda J, Fischer FD, Fratzl P (2004) Modelling of kinetics in multi-component multi-phase systems with spherical precipitates: II: numerical solution and application. *Mater Sci Eng A* 385(1–2):157
 37. Apel M, Böttger B, Rudnizki J, Schaffnit P, Steinbach I (2009) Grain growth simulations including particle pinning using the multiphase-field concept. *ISIJ* 49(7):1024–1029
 38. Rudnizki J, Zeislmair B, Prah U, Bleck W (2010) Prediction of abnormal grain growth during high temperature treatment. *Comp Mater Sci* 49(2):209
 39. Jansen U (2009) Simulation des Schweißens kleiner Bauteile”. Diplomarbeit, Lehrstuhl: Nichtlineare Dynamik der Laserfertigungsverfahren, RWTH Aachen
 40. www.magmasoft.de
 41. Apel M, Benke S, Steinbach I (2009) Virtual dilatometer curves and effective young’s modulus of a 3D multiphase structure calculated by the phase-field method. *Comp Mater Sci* 45(3):589
 42. Benke S (2008) A Multi-phase-field model including inelastic deformation for solid state transformations. *Proceedings in Applied Mathematics and Mechanic* 8(1):10407